Т. 88, № 3 **ЖУРНАЛ ПРИКЛАДНОЙ СПЕКТРОСКОПИИ** МАЙ — ИЮНЬ 2021
V. 88, N 3 **JOURNAL OF APPLIED SPECTROSCOPY** MAY — JUNE 2021

INVESTIGATION OF THE PHYSICAL PROPERTIES OF EUCALYPTUS AND *Pinus halepensis* ESSENTIAL OILS USING DIELECTRIC SPECTROSCOPY AND GAS CHROMATOGRAPHY-MASS SPECTROMETRY[**]

**O. Harrouz [1,2*], F. Frenzel [3], O. Mosbah [1], S. M. Terrah [1],
F. Z. Sabi [1], A. Sahila [1], N. Zekri [1], F. Kremer [3]**

[1] University Oran, Laboratory of Material Physics, Algeria; e-mail: omar47203@gmail.com
[2] ENS, Ouargla, Algeria
[3] University of Leipzig, Faculty of Physics and Geosciences, 04103 Leipzig, Germany

The gas chromatography-mass spectrometry and dielectric spectroscopy techniques are used to characterize the thermodynamic properties of the essential oils extracted from two main Mediterranean wildland fuels, namely eucalyptus leaves and Pinus halepensis needles. These oils are assumed to be representative of the fuels organic volatile components that exhibit different fire behaviors. The relaxation frequencies determined from the peak of the imaginary permittivity spectra using the Havriliak–Negami empirical law revealed the Arrhenius dependence on temperature. Two activation energies are obtained: the first is around 4.13 kJ /mol for both species, and the second activation energy is around 1.27 kJ/mol for the Pinus halepensis essential oil and around 2.15 kJ/mol for the eucalyptus essential oil. Qualitative and quantitative composition differences are observed with GC-MS measurements for eucalyptus leaves and Pinus halepensis needles essential oils.

Keywords: *dielectric spectroscopy, gas chromatography-mass spectrometry, essential oils-wildfires.*

ИССЛЕДОВАНИЕ ЭФИРНЫХ МАСЕЛ ЭВКАЛИПТА И *Pinus halepensis* МЕТОДАМИ ДИЭЛЕКТРИЧЕСКОЙ СПЕКТРОСКОПИИ И ГАЗОВОЙ ХРОМАТОГРАФИИ-МАСС-СПЕКТРОМЕТРИИ

**O. Harrouz [1,2*], F. Frenzel [3], O. Mosbah [1], S. M. Terrah [1],
F. Z. Sabi [1], A. Sahila [1], N. Zekri [1], F. Kremer [3]**

УДК 543.42;543.544

[1] Университет Орана, Алжир; e-mail: omar47203@gmail.com
[2] ENS, Уаргла, Алжир
[3] Лейпцигский университет, 04103 Лейпциг, Германия

(Поступила 8 августа 2019)

Методы газовой хроматографии-масс-спектрометрии и диэлектрической спектроскопии использованы для характеризации термодинамических свойств эфирных масел, извлеченных из двух основных источников возгорания лесов в Средиземноморье, а именно листьев эвкалипта и игл сосны алеппской. Эти масла представляют собой летучие органические компоненты, которые по-разному проявляются при пожаре. Частоты релаксации, определенные по пику мнимых спектров диэлектрической проницаемости с использованием эмпирического закона Гавриляка–Негами, выявили зависимость Аррениуса от температуры. Получены энергии активации: ~4.13 кДж/моль для обоих видов, ~1.27 и 2.15 кДж/моль для эфирных масел сосны алеппской и эвкалипта. Качественные и количественные различия в составе эфирных масел листьев эвкалипта и игл сосны подтверждаются с помощью измерений методом газовой хроматографии-масс-спектрометрии.

[**] Full text is published in JAS V. 88, No. 3 (http://springer.com/journal/10812) and in electronic version of ZhPS V. 88, No. 3 (http://www.elibrary.ru/title_about.asp?id=7318; sales@elibrary.ru).

Ключевые слова: *диэлектрическая спектроскопия, газовая хроматография-масс-спектрометрия, эфирные масла, лесные пожары.*

Introduction. The chemical composition of a plant and its moisture content determine the delay time before ignition and fire spread [1]. The emitted volatile organic components (VOCs) during the fuel heating process might lead to a generalized conflagration, in particular wildland conflagrations [2–4]. Most Mediterranean species produce highly flammable volatiles such as monoterpenes. The flammability of fuels is correlated to their monoterpenoids content [5–8]. Hence, it is important to identify the major organic components involved in wildfire fuel flammability. The gas chromatography technique coupled with mass spectrometry (GC-MS) is the most used technique for this [9]. One of the most recent experimental methods for the characterization of materials is dielectric spectroscopy. This technique is known to be simple, fast, and nondestructive. However, it is very difficult to use this technique to investigate VOCs in their gaseous phase. Hence, it is easier to use essential oils whose components are assumed to be representative of VOCs [10].

Pinus halepensis needles – the most available fuel in Algeria – are among the major fuels affected by wildfire in this country. Indeed, they are known to exhibit a high fire susceptibility index, contrary to *eucalyptus leaves* that are less easily flammable but, nevertheless, contributed significantly to the extreme wildfires of 2017 in Portugal (where they are the major fuel) [11–19].The identification of the composition of the oils extracted from these fuels using the GC-MS technique and the characterization of the oils thermodynamic properties using dielectric spectroscopy are the aims of the present work.

Materials and methods. *Eucalyptus leaves* (EU) and *Pinus halepensis* (PH) needles were harvested from the Campus of USTO University, near the LEPM Laboratory of Material Physics (Oran, Algeria). The experimental design of this work is composed of three steps: oil extraction**,** measurement of oil dielectric spectra, and chromatograph-mass spectroscopy.

Oil extraction. The extraction was performed by the hydrodistillation technique, where 300 g of PH needles and EU leaves were used separately in 3 L of water during 4 h. The principle of this hydrodistillation, which is the simplest and oldest technique used for oil extraction, corresponds to heterogeneous distillation involving Dalton's and Raoult's laws [19]. The process consists of immersing the plant raw material in a flask filled with water placed on a heat source until boiling. The heat allows the bursting of plant cells and the release of odorous molecules contained in the plant materials. These aromatic molecules form an isotropic mixture with the water vapor [20–23]. The released vapor is condensed in a refrigerant, and the essential oil is separated from water by density difference with the use of the Clevenger device [24].

Measurement of oil dielectric spectra. The dielectric spectral measurements were realized mainly at IEP (University of Leipzig, Germany), using a Novocontrol high-resolution dielectric Alpha A10 analyser (preliminary measurements were realized at LEPM with the same equipment at room temperature) [25, 26]. The sample cell was formed by 0.1 mm silica spacers attached to the lower electrode, on which a drop of 1 ml of essential oil is placed. The upper electrode is then set, and the assembly is fixed on the module BDS 1200 of the dielectric analyser (Fig. 1).

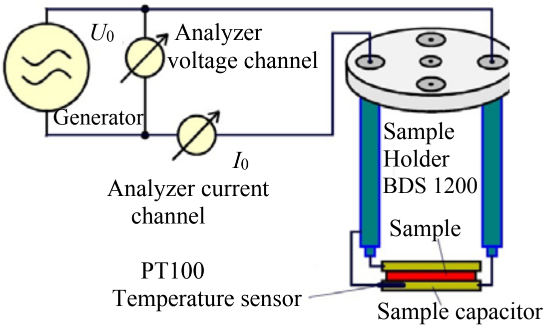

Fig. 1. Principle of dielectric or impedance measurement.

The complex dielectric function

$$\varepsilon^*(\omega) = \varepsilon'(\omega) - i\varepsilon''(\omega), \tag{1}$$

where ω denotes the frequency, ε′ and ε″ represent the real and imaginary part of the complex dielectric function, and i symbolizes the imaginary unit ($i^2 = -1$), was measured by varying the temperature in the range 100–300 K, while the frequency ranged from 10^{-2} to 10^6 Hz.

Various empirical models can be used to describe either the time or the frequency dependence of the complex dielectric permittivity of polar liquids like essential oils. In the time domain, the stretched exponential empirical law is generally used, whereas in the frequency domain, the general relaxation model of Havriliak and Negami (HN) is usually chosen [27]:

$$\varepsilon^*_{\mathrm{HN}}(\omega) = \varepsilon_\infty + \frac{\Delta\varepsilon}{(1 + (i\omega\tau_{\mathrm{HN}})^\beta)^\gamma}, \tag{2}$$

where $\Delta\varepsilon = \varepsilon_s - \varepsilon_\infty$ is the dielectric strength with $\varepsilon_s = \varepsilon(0)$ and $\varepsilon_\infty = \varepsilon(\infty)$. The relaxation time in the HN model (2) is τ_{HN}, and the exponents β and γ describe respectively the symmetric (Cole and Cole) and asymmetric (Cole and Davidson) broadening of the complex dielectric function compared to the half-circle of the Debye model. These exponents are less than unity. These broadenings depend on the distribution of the relaxation time in the material [28, 29]. The Debye model is recovered with $\beta = \gamma = 1$. Contrary to the Debye model, where the maximum strength of the imaginary part of the dielectric permittivity (loss) corresponds to the relaxation time, the maximum loss for the HN model is fitted at a frequency $f_{\max}$ that is related to τ_{HN} by [30]:

$$f_{\max} = \frac{\omega}{2\pi} = \frac{1}{2\pi\tau_{\mathrm{HN}}} \sin\left(\frac{\pi\beta}{2+2\gamma}\right)^{1/\beta} \sin\left(\frac{\pi\beta\gamma}{2+2\gamma}\right)^{-1/\beta}. \tag{3}$$

Chromatographic analysis. A sample of each extracted essential oil was analyzed using a Bruker gas chromatography model equipped with a DB-5 capillary column and a Varian Saturn 2000 ion trap mass detector. The GC-MS was operated under the following conditions: column length 30.00 mm; column diameter 0.250 mm; gas He; flowrate 37 cm/s; injection 1 μL; inject type split; inject temperature 250°C; split fellow 60 ml/min; pressure 7 psi.

The identification of the constituents was based on the comparison of the retention times with those of the authentic compounds, comparing their linear retention indices relative to the series of n-hydrocarbons, and on computer matching against The National Institute of Standards and Technology (NIST) and homemade library mass spectra built up from pure substances and components of the known oils and the MS literature data of Adams [31–37].

Results and discussion. *Dielectric measurements of the extracted essential oils.* The experimental results of the imaginary part ε'' for the two species are presented in Figs. 2a,b as a function of frequency at different temperatures. For the selected temperatures the dielectric loss spectra are dominated by a huge increase in ε'' towards low frequencies for both species. This behavior is ascribed to the conductivity contributions of the electrodes, which is assumed constant, e.g., a frequency-independent conductivity, $\sigma(\omega) = \sigma_{\mathrm{dc}}$, leading to the power-law behavior $\varepsilon'' \sim \sigma_{\mathrm{dc}}/\omega$. Beyond the effect of the electrodes shown at low frequencies, the relaxation process corresponds to the maximum value of ε''. This maximum is shifted towards higher frequencies with increasing temperature. For both species, this relaxation process is not observed above 270 K. In Figs. 2c,d the imaginary part ε'' is plotted for only the temperatures where the relaxation process is clearly observed. In both figures, an asymmetric behavior appears with two different slopes on each side of the spectrum. Therefore, the relaxation process is characterized by a distribution of the relaxation frequency as expected, and the parameters can be fitted using the HN model.

The spectra in Figs. 2c,d revealed well-developed relaxation peaks, shifting through the frequency window with temperature. At 185 K it seems that the PH oil spectrum exhibits three relaxation processes and only two processes for the EU oil. Now let us investigate the activation energies of phase transitions for these species by analyzing their temperature-dependent HN fitted relaxation frequency. Two different laws are known for the temperature dependence of the relaxation time: the Arrhenius for single activation energy and the Vogel–Fulcher–Tammann (VFT) laws describing multiple activation energy [30]:

$$\tau_{\max}(T) = \begin{cases} \tau_0 \exp(E_a / RT), & \text{Arrhenius,} \\ \tau_0 \exp[DT_0 / (T - T_0)], & \text{VFT,} \end{cases} \tag{4}$$

where E_a is the activation energy, R is the gas constant, τ_0 is a pre-exponential factor, T_0 is the Vogel temperature, and D is called the “fragility” parameter and provides a quantitative measure of the deviation from the Arrhenius law. The activation plot ($-\log\tau_{\max}$ vs. $1000/T$) is shown in Fig. 3 for the PH and EU oils. A linear trend corresponds to the Arrhenius law.

The two relaxation processes of the EU oil and the first process of the PH oil seem clearly well described by Arrhenius [28]. The second process for the PH oil is ignored in this analysis because it cannot be well fitted in Fig. 2c,d. Finally, due to the lack of data, the third process of the PH oil may either follow the VFT model or the Arrhenius law. If the Arrhenius behavior is fitted for all processes, the activation energies are shown in Table 1. From the results presented in Table 1, the same first activation energy observed for the PH and EU essential oils is a signature of common components in these oils. The second activation energy of the PH essential oil seems smaller than that of the EU oil, which indicates that some non-common components may have smaller phase transition energy for the PH oil than the EU one. Differential scanning calorimetry measurements may identify the phase transition temperatures related to these activation energies. Note in a similar way that the critical ignition energy of the PH needles was found to be much smaller than that of the EU leaves, although the ignition phase transition occurs at higher temperatures than that of the measured second activation energy appearing in Table 1 [38]. The components responsible for the second activation energy might be the major components contributing to the ignition process.

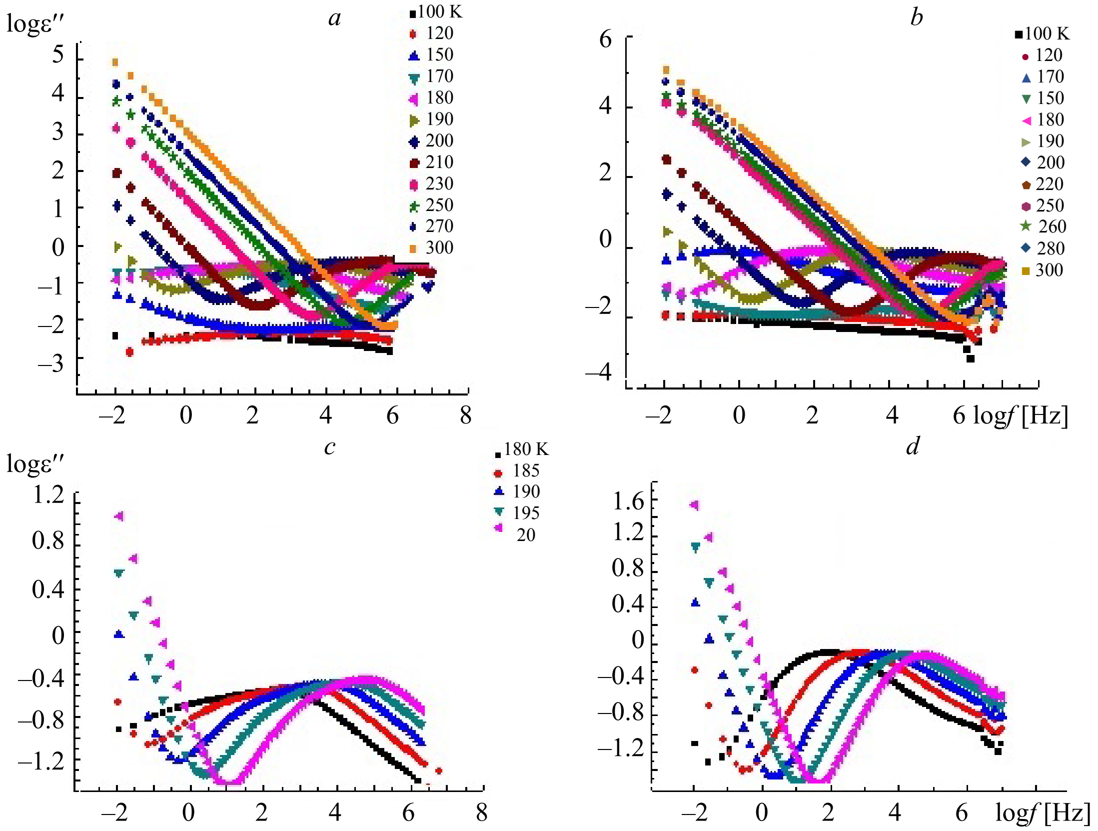

Fig. 2. ε″ vs. ω presented for selected temperature for PH (a, c) and EU (b, d).

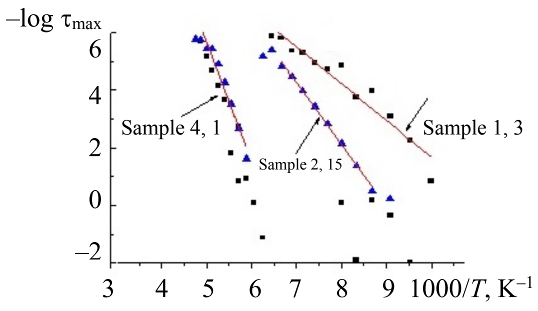

Fig. 3. Activation plot of the HN fitted relaxation time for PH (■) and EU (▲) oils.

TABLE 1. Activation Energies of the PH and EU Oils Estimated from the Arrhenius Model

Essential oil	E_{a1}, kJ/mol	E_{a2}, kJ/mol
EU	4.13	2.15
PH	4.13	1.27

GC-MS of the extracted essential oils. The above-discussed contribution of the oils components to various phase transitions led us to investigate the composition of the two essential oils. The GC-MS technique is the most common method, where the amounts of the components from the oil are determined by the peak area normalization method. The retention time (Rt), molecular formula (MF), and concentration percentage (%) of chemical constituents of the two essential oils of EU and PH are listed in Table 2.

TABLE 2. Composition of the Main Components of the EU and PH Essential Oils

Compound	MF	Rt(EU)	Rt(PH)	EU, %	PH, %
α-Pinene	$C_{10}H_{16}$	7.511	7.71	2.34	1.69
β-Pinene	$C_{10}H_{16}$	11.98	12.28	1.36	10.44
p-Cymene	$C_{10}H_{14}$	15.67	–	15.75	–
1,8-Cineole	$C_{10}H_{16}$	16.56	–	25.21	–
γ-Terpinene	$C_{10}H_{16}$	19.08	–	2.12	
β-cis-Ocimene	$C_{10}H_{16}$	–	18.36	–	1.15
α-Terpinolene	$C_{10}H_{16}$	–	22.07	–	4.52
Caryophyllene	$C_{15}H_{24}$	–	46.78	–	7.58
Humulene	$C_{15}H_{24}$	–	48.88	–	2.13
Phenethylisovalerate	$C_{13}H_{18}O_2$	–	51.62	–	12.51
Caryophyllene oxide	$C_{15}H_{24}O$	–	56.48	–	1.39
Cembrene	$C_{20}H_{32}$	–	74.59	–	1.76
Thunbergol	$C_{20}H_{34}O$	80.11	80.15	2.86	5.67
bis(2-Ethylhexyl)phthalate	$C_{24}H_{38}O_4$	101.16	100.92	15.285	18.98

After the comparison of the results, some qualitative and quantitative differences in the compositions of the oils were observed. In the essential oils of the PH needles, the principal constituent was bis(2-ethylhexyl)phthalate (18.98%), followed by phenethylisovalerate (12.51%) and β-pinene (10.44%). 1,8-Cineole appears as the main compound (25.21%) of the EU essential oil, followed by *p*-cymene (15.75%), and bis(2-ethylhexyl)phthalate (15.28%). The PH essential oil seems to be more heterogeneous compared to the EU essential oil. Actually, β-pinene, known for its high flammability [2, 3], is among the major compounds in the PH essential oil compared to the EU essential oil, where its composition is ten times smaller (Table 2). This composition difference of β-pinene can explain the relatively high flammability of the emitted VOCs by the PH needles compared to the EU leaves.

Conclusions. The essential oils of *Eucalyptus leaves* and *Pinus halepensis* needles extracted by hydrodistillation were analyzed using dielectric spectroscopy and GC-MS analysis. Despite the effect of electrodes, the frequency dependence of ε″ at a low frequency for the two essential oils at different temperatures (above 270 K) shows two relaxation processes for each essential oil. The model of Havriliak and Negami fitted relaxation frequencies revealed the Arrhenius behavior with two activation energies for each oil. The first activation energy is around 4.13 kJ/mol identically for both essential oils. The second activation energy of the *Pinus halepensis* essential oil is around 1.27 kJ/mol, much smaller than that of the *Eucalyptus leaves* essential oil, which is around 2.15 kJ/mol. The differential scanning calorimetry technique is expected to explain the nature of phase transitions related to the activation energies of these essential oils. The GC-MS analysis of the *Pinus halepensis* and *Eucalyptus leaves* essential oils revealed that 1,8-cineole is the major component of the *Eucalyptus leaves* essential oil, whereas the *Pinus halepensis* essential oil seems more heterogeneous, with three major components. β-Pinene appears to be among the major components of the *Pinus halepensis* essential oil but is a minor component in the *Eucalyptus leaves* essential oil. This component is known to have high flammability properties. This could explain the flammability difference between *Pinus halepensis* needles and *Eucalyptus leaves*.

REFERENCES

1. J. H. Balbi, F. Morandini, X. Silvani, J. B. Filippi, F. Rinieri, *Combust. Flame*, **156**, 2217–2230 (2009).
2. K. Chetehouna, T. Barboni, I. Zarguili, E. Leoni, A. Simeoni, A. C. Fernandez-Pello, *Combust. Sci. Technol.*, **181**, No. 10, 1273–1288 (2009).
3. L. Courty, K. Chetehouna, J. P. Garo, D. X. Viegas, In: *A volatile Organic Compounds Flammability Approach for Accelerating Forest Fires, Modelling, Monitoring and Management of Forest Fires II*, Eds. Perona & Brebbia, WIT Transactions on Ecology and the Environment, 137 (2010).
4. G. A. Alessio, J. Peñuelas, J. Llusià, R. Ogaya, M. Estiarte, De Lillis, *Int. J. Wildland Fire*, **17**, No. 2, 274–286 (2008), doi:10.1071/WF07038.
5. G. Massari, A. Leopaldi, *Plant Biosyst.*, **132** (1998).
6. L. Catoire, V. Naudet, *Proc. Safety Prog.*, **24**, 130–137 (2005)
7. E. Von Rudloff, *Can. J.*, **53**, 2978–2982 (1975).
8. J. P. Greenberg, H. Friedli, A. B. Guenther, D. Hanson, P. Harley, T. Karl, *Atmos. Chem. Phys.*, **6**, 81–91 (2006).
9. A. Koedam, In: *Capillary Gas Chromatography in Essential Oils Analysis*, Eds. P. Sandra, C. Bicchi, Huethig, Heidelberg (1987).
10. S. D. Romano, P. A. Sorichetti, *Dielectric Relaxation Spectroscopy in Biodiesel Production and Characterization*, Springer Verlag, London (2011).
11. J. Llusià, J. Peñuelas, *Am. J. Bot.*, **87**, 133–140 (2000).
12. C. S. White, *J. Chem. Ecol.*, **20**, 1381–1406 (1994), doi:10.1007/BF02059813.
13. M. K. Owens, C. D. Lin, C. A. Taylor, Jr., S. G. Whisenant, *J. Chem. Ecol.*, **24**, No. 12, 2115–2129 (1998).
14. J. Tranchant, *Manuel Pratique de Chromatographie en Phase Gazeuse*, Masson et Cie, Paris (1982).
15. D. Alexandrian, E. Rigolot, *Sensibilité du pin d'Alep à l'incendie, Forêt méditerranéenne*, 3 (1992).
16. www.foret-mediterraneenne.org/fr/catalogue (2008).
17. Alvarez, M. Gracia, J. Vayreda, J. Retana, *Forest Ecol. Manage.*, 270 (2012).
18. M. Häusler, J. P. Nunes, P. Soares, J. M. Sánchez, J. M. N. Silva, T. Warneke, J. J. Keizer, J. M. C. Pereira, *Int. J. Remote Sens.*, **39**, 6499–6524 (2018).
19. D. L. Pavida, G. M. Lampman, G. S. Kriz, In: *Introduction to Organic Laboratory Techniques*, Ed. W. B. Sauders, Philadelphia, USA (1976).
20. J. F. Clevenger, *American Perfumer & Essential Oil Review*, 467–503 (1928).
21. M. Gorunovic, N. Mimica-Dukic, G. Kite, D. Stosic, *Pharmazie*, **47**, H8 (1992).
22. K. Hannus, G. Pensar, *Phytochemistry*, **13**, 2563–2566 (1974).
23. E. Bocchio, *Parfums, Cosmetiques, Aromes*, **63**, 61–62 (1985).
24. J. F. Clevenger, *J. Ann. Pharm. Assoc.*, **17**, No. 4, 346–351 (1928).
25. Novocontrol Technologies GmbH & Co. KG, POT/GAL 15V 10A Electrochemical Impedance Potentiostat Galvanostat Test Interface for Alpha-A Analyzer, User's manual.
26. Novocontrol Technologies GmbH & Co. KG, Novotherm-HT High Temperature Control Systems 650, 800, 1000, 1200, and 1400, User's manual.
27. S. Havriliak, Negami, *Polymer*, **8**, 161 (1967).
28. J. Ross, J. R. Macdonald, *Impedance Spectroscopy: Theory, Experiment and Application*, Wiley (2005).
29. A. Schönhals, F. Kremer, E. Schlosser, *Phys. Rev. Lett.*, **67**, 999 (1991).
30. F. Kremer, In: *Broadland Dielectric Spectroscopy*, Ed. A. Schönhals, Springer, Heidelberg (2002).
31. P. Henning, A. Steinborn, W. Engewald, *Chromatographia*, **3**, 689–694 (1994).
32. P. Arpino, A. Prévôt, J. Serpinet, J. Tranchant, A. Vergnol, P. Witier, In: *Manuel Pratique de Chromatographie en Phase Gazeuse*, Ed. Masson, Paris (1995).
33. G. Castello, *J. Chromatogr. A*, **842**, 51–64(1999).
34. A. J. Handley, E. R. Adlard, *Gas Chromatographic Techniques and Application,* Sheffield Academic, London, 12, Thermo Fisher Scientific (2011).
35. G. A. Eiceman, In: *Encyclopedia of Analytical Chemistry: Applications, Theory, and Instrumentation*, Ed. R. A. Meyers, Wiley, Chichester (2000).
36. F. G. Kitson, B. S. Larsen, C. N. McEwen, *Gas Chromatography and Mass Spectrometry: a Practical Guide*, Academic Press, Boston (1996)
37. W. M. A. Niessen, *Current Practice of Gas Chromatography–Mass Spectrometry*, Marcel Dekker, New York (2001).
38. F. Z. Sabi, *Fire Safety J.*, **119**, 103257 (2021), doi: 10.1016/j.firesaf.2020.103257.